AMERICAN SOCIETY FOR MICROBIOLOGY | Journal of Virology®

VIRUS-CELL INTERACTIONS

A Genome-Wide CRISPR-Cas9 Screen Identifies the Dolichol-Phosphate Mannose Synthase Complex as a Host Dependency Factor for Dengue Virus Infection

Athena Labeau,[a] Etienne Simon-Loriere,[b] Mohamed-Lamine Hafirassou,[a] Lucie Bonnet-Madin,[a] Sarah Tessier,[a] Alessia Zamborlini,[a,c] Thierry Dupré,[d] Nathalie Seta,[d] Olivier Schwartz,[e] Marie-Laure Chaix,[a,f] Constance Delaugerre,[a,f] Ali Amara,[a] Laurent Meertens[a]

[a]INSERM U944, CNRS UMR 7212, Genomes & Cell Biology of Disease Unit, Institut de Recherche Saint-Louis, Université de Paris, Hôpital Saint-Louis, Paris, France
[b]G5 Evolutionary Genomics of RNA Viruses, Institut Pasteur, Paris, France
[c]Institute for Integrative Biology of the Cell (I2BC), CEA, CNRS, Université Paris-Sud, Université Paris-Saclay, Gif-sur-Yvette, France
[d]Laboratoire de Biochimie, Hôpital Bichat-Claude Bernard, Paris, France
[e]Institut Pasteur, Virus and Immunity Unit, CNRS-UMR3569, Paris, France
[f]Laboratoire de Virologie et Département des Maladies Infectieuses, Hôpital Saint-Louis, APHP, Paris, France

ABSTRACT Dengue virus (DENV) is a mosquito-borne flavivirus responsible for dengue disease, a major human health concern for which no specific therapies are available. Like other viruses, DENV relies heavily on the host cellular machinery for productive infection. In this study, we performed a genome-wide CRISPR-Cas9 screen using haploid HAP1 cells to identify host genes important for DENV infection. We identified DPM1 and -3, two subunits of the endoplasmic reticulum (ER) resident dolichol-phosphate mannose synthase (DPMS) complex, as host dependency factors for DENV and other related flaviviruses, such as Zika virus (ZIKV). The DPMS complex catalyzes the synthesis of dolichol-phosphate mannose (DPM), which serves as mannosyl donor in pathways leading to N-glycosylation, glycosylphosphatidylinositol (GPI) anchor biosynthesis, and C- or O-mannosylation of proteins in the ER lumen. Mutation in the DXD motif of DPM1, which is essential for its catalytic activity, abolished DPMS-mediated DENV infection. Similarly, genetic ablation of ALG3, a mannosyltransferase that transfers mannose to lipid-linked oligosaccharide (LLO), rendered cells poorly susceptible to DENV. We also established that in cells deficient for DPMS activity, viral RNA amplification is hampered and truncated oligosaccharides are transferred to the viral prM and E glycoproteins, affecting their proper folding. Overall, our study provides new insights into the host-dependent mechanisms of DENV infection and supports current therapeutic approaches using glycosylation inhibitors to treat DENV infection.

IMPORTANCE Dengue disease, which is caused by dengue virus (DENV), has emerged as the most important mosquito-borne viral disease in humans and is a major global health concern. DENV encodes only few proteins and relies on the host cell machinery to accomplish its life cycle. The identification of the host factors important for DENV infection is needed to propose new targets for antiviral intervention. Using a genome-wide CRISPR-Cas9 screen, we identified DPM1 and -3, two subunits of the DPMS complex, as important host factors for the replication of DENV as well as other related viruses such as Zika virus. We established that DPMS complex plays dual roles during viral infection, both regulating viral RNA replication and promoting viral structural glycoprotein folding/stability. These results provide insights into the host molecules exploited by DENV and other flaviviruses to facilitate their life cycle.

Citation Labeau A, Simon-Loriere E, Hafirassou M-L, Bonnet-Madin L, Tessier S, Zamborlini A, Dupré T, Seta N, Schwartz O, Chaix M-L, Delaugerre C, Amara A, Meertens L. 2020. A genome-wide CRISPR-Cas9 screen identifies the dolichol-phosphate mannose synthase complex as a host dependency factor for dengue virus infection. J Virol 94:e01751-19. https://doi.org/10.1128/JVI.01751-19.

Editor Mark T. Heise, University of North Carolina at Chapel Hill

Address correspondence to Ali Amara, ali.amara@inserm.fr, or Laurent Meertens, laurent.meertens@inserm.fr.

Received 11 October 2019
Accepted 20 December 2019
Accepted manuscript posted online 8 January 2020
Published 17 March 2020

KEYWORDS dengue fever, dengue virus, N-glycosylation, Zika virus, dolichol-phosphate mannose, glycoprotein folding

Dengue is the most prevalent arthropod-borne viral disease that is caused by the four dengue virus (DENV) serotypes (DENV1 to -4). DENV belongs to the *Flavivirus* genus of the *Flaviviridae* family, which includes important emerging and reemerging viruses such as West Nile virus (WNV), yellow fever virus (YFV), Zika virus (ZIKV), and tick-borne encephalitis virus (TBEV) (1). DENV is transmitted by the bite of *Aedes* mosquitoes and may cause diseases ranging from mild fever to lethal dengue hemorrhagic fever and dengue shock syndrome (2). Recent estimation suggests that half the world's population lives in areas where dengue fever is endemic (3), with 100 million symptomatic infections and 500,000 cases of the severe manifestations of the disease per year (4). There are currently no antiviral therapies against DENV, and the recently approved tetravalent lived-attenuated vaccine showed relative efficacy depending on (i) the serostatus at the time of vaccination and (ii) the infecting serotype, with a higher rate of efficacy toward DENV3 and -4 (5, 6).

DENV is an enveloped virus containing a positive-stranded RNA genome of ~11 kb. Upon entry into the target cell, the viral genome is translated by the host cell machinery into a large polyprotein precursor, which is subsequently processed by host and viral proteases into three structural proteins, i.e., C (core), prM (precursor of the M protein), and E (envelope) glycoproteins, and seven nonstructural (NS) proteins called NS1, NS2A, NS2B, NS3, NS4A, NS4B, and NS5 (7). The structural proteins form the virus particles, whereas the NS proteins play a central role in viral replication, assembly, and the modulation of innate immune responses (8). As an obligate intracellular parasite, DENV depends heavily on the host cell machinery to accomplish its infectious life cycle. Recent genome-wide loss-of-function CRISPR-Cas9 screens have led to the identification of host molecules essential for DENV infection (9–11). Consistent with the critical role of the endoplasmic reticulum (ER) in flavivirus infection (12), such studies identified as major hits components of ER resident multiprotein complexes. These include the oligosaccharyltransferase complex (OST), which catalyzes the transfer of high-molecular-weight mannose oligosaccharides to nascent proteins during N-glycosylation (13); the ER membrane protein complex (EMC), which functions both as a chaperone for multipass transmembrane proteins (14) and as an insertase for tail-anchored membrane proteins (15); and the translocon and translocon-associated protein (TRAP) complex, which regulates the transport across or insertion into the ER membranes of proteins synthetized by ER-bound ribosomes (16). More recently, a comprehensive identification of RNA-binding proteins by mass spectrometry (ChIRP-MS) coupled with genome-wide CRISPR-Cas9 screens for all four DENV serotypes identified HDLBP and RRBP1, two ER-associated RNA-binding proteins, as important factors in DENV RNA translation and replication (11). Interestingly, many of these genes were also highly enriched in independent genetic screens for related flaviviruses, such as WNV and ZIKV (17–19). Although these studies undeniably identified a core set of host factors essential for DENV biology, these CRISPR-Cas9 screens were performed in cell lines (Huh7.5.1 and 293T) with diploid or hyperploid genomes, leaving open the possibility that additional cellular genes important for viral replication have been overlooked. In the present study, we performed a pooled genome-wide CRISPR-Cas9 screen in the near-haploid HAP1 cells to identify host factors required for DENV infection. Our unbiased approach identified the DPM1 and DPM3 molecules, two subunits of the dolichol-phosphate mannose synthase complex (DPMS), as DENV host dependency factors. We found that DPMS is required for both optimal viral RNA amplification and proper glycosylation and folding of viral structural proteins prM and E.

RESULTS AND DISCUSSION

DPM1 and -3 are host factors for DENV infection. To identify host factors required for DENV infection, we performed a CRISPR-Cas9 genome-wide screen in the HAP1 haploid cell line. We transduced HAP1 cells with the human GeCKO v2 single guide RNA

(sgRNA) libraries A and B, which contain each 3 unique sgRNAs targeting 19,050 genes (20). Parental cells and cells expressing the gRNA libraries were inoculated with the DENV2 primary strain Jamaica (JAM) at a multiplicity of infection (MOI) of 5. After 2 weeks, surviving clones were detected among library-transduced cells but not in parental cells (Fig. 1A). Genomic DNA from cells that survived to DENV2 JAM infection was extracted and the integrated sgRNAs were amplified by PCR and sequenced. Gene enrichment was assessed using MAGeCK software as previously described (21) (Table 1). Among our 17 top candidates (false-discovery rate [FDR] $<$ 0.05), 8 hits were found in recent flavivirus CRISPR-Cas9 screens, such as members of the translocon and TRAP complex (SEC61A1 and SSR3), OST (STT3A, STT3B, and RPN2) and ECM (EMC6) complexes and proteins involved in heparan sulfate biosynthesis (EXTL3 and EXT2) (Fig. 1B) (9, 10, 18, 19). We additionally identified uncharacterized host factors involved in the synthesis of glycosaminoglycans (B4GALT7, B3GALT6, and B3GAT3) and the sulfonation pathway (PAPSS1 and SLC35B2) (Fig. 1B). Genes encoding DPM1 and -3 were also significantly enriched in our screening (Fig. 1B) and were never characterized as virus host factors. DPM1 and -3 are two subunits of the dolichol-phosphate mannose (DPM) synthase complex (DPMS), which transfers a mannose residue from the GDP-mannose donor to the dolichol-phosphate carrier (22). In the ER lumen, DPM serves as a mannosyl donor in pathways leading to the glycosylphosphatidylinositol (GPI) anchor biosynthesis, N-glycosylation, and O- and C-mannosylation of cellular proteins (23). To validate the importance of DPM1 and -3 as DENV host factors, we edited the corresponding genes in both HAP1 and 293T cells (DPM1^{KO} or DMP3^{KO}) using CRISPR-Cas9. DPM gene ablation was confirmed by both genomic DNA sequencing (Fig. 1C) and Western blot analysis (Fig. 1D). We also measured the cell surface levels of GPI-anchored CD59 as a manner to monitor DPMS activity and established that they were undetectable in both DPM1- and -3-deficient cells (Fig. 1E). Consistent with previous results (24), we observed a lack of expression of DPM1, the catalytic subunit of the DPMS complex, in the absence of DPM3, which is known to tether DPM1 at the ER membrane (Fig. 1D). We then performed a CellTiter-Glo assay to ascertain that DPM1 and -3 deficiency had no impact on cell viability and growth (Fig. 1F). DENV2 JAM infection was severely impaired upon editing of either DPM1 or -3, as shown by both the reduced numbers of cells positive for intracellular prM and NS3 proteins (Fig. 1G and H) and the absence of detectable levels of progeny viruses released in the culture supernatants (Fig. 1I). Importantly, *trans*-complementation of the HAP1 or 293T knockout (KO) cells with human DPM1 or DPM3 cDNA restored DPMS activity, as assessed by quantifying CD59 at the cell surface, and rescued cell susceptibility to DENV infection (Fig. 2A to C). Similarly, DPM1 and DPM3 depletion in Huh-7 and primary foreskin fibroblasts resulted in less DENV infection than in control cells (Fig. 2D and E). This demonstrates that loss of DPM1 or DPM3 is solely responsible for the observed virus resistance phenotype.

To determine whether DPM1 and -3 mediate infection by other DENV serotypes, we challenged both DPM1^{KO} and DMP3^{KO} cells with DENV1, DENV3, and DENV4 primary isolates or the laboratory-adapted strains DENV2 New Guinea C (NGC) and DENV2 Thaïland/16681/84 (16681). We found that all DENV serotypes required the presence of DPM1 or -3 for efficient infection (Fig. 3A and B). In addition, infection by ZIKV and YFV 17D, two related flaviviruses, was significantly inhibited in cells lacking DPM1 or -3, whereas infection by vesicular stomatitis virus G protein (VSV-G)-pseudotyped HIV (VSVpp) was unaffected (Fig. 3C and D). It is noteworthy that several MOIs were used to cover the linear range of infection for each virus. Altogether, these data showed that DPM1 and -3 are important host factors for DENV and other related flaviviruses.

The catalytic activity of DPM1 is required for efficient DENV infection. DPM1 is the catalytic subunit of the human DPMS complex (25). Recent resolution of the crystal structure of an archaeal DPMS complex bound to the donor substrate highlighted the role of two aspartic residues within a conserved DAD motif of the catalytic pocket, which is a molecular signature of DPMS complexes in several species (26) (Fig. 4A). To investigate whether DPM1 catalytic activity regulates DENV infection, we designed

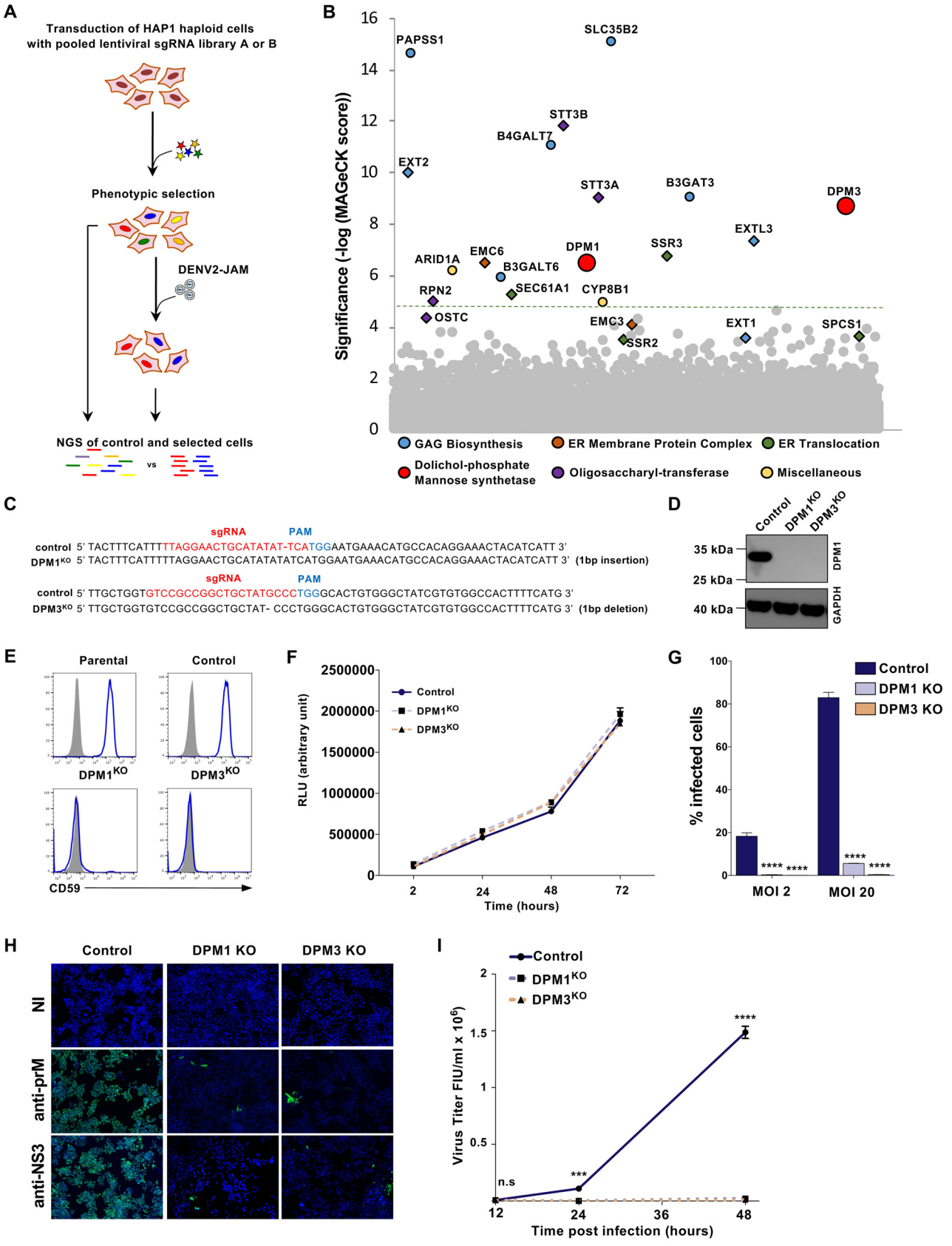

FIG 1 Haploid CRISPR-Cas9 screen identifies DPM1 and -3 as host factors for DENV infection. (A) Schematic representation of the CRISPR-Cas9 screen to identify host factors for DENV2 JAM in HAP1 cells. (B) Results of the DENV2 JAM screen analyzed by MAGeCK. Each circle represents individual gene.

(Continued on next page)

DPM1 variants mutated in the DAD sequence (Fig. 4A, D118A and D120A) and stably expressed them in DPM1^{KO} HAP1 cells. Western blot analysis showed that DPM1 D118A and D120A were expressed at levels similar to those in the wild-type (WT) protein (Fig. 4B). Notably, neither the D118A nor D120A DPM1 mutant was able to restore CD59 cell surface expression, indicating that these proteins are catalytically dead (Fig. 4C). Furthermore, infection studies showed that none of the catalytic mutants could rescue the infection of DPM1^{KO} cells by DENV, whatever the MOI used (Fig. 4D). Together, these data indicated that integrity of the DPM1 catalytic motif DAD, and therefore synthesis of DPM, is important for DENV infection.

Transfer of mannose from DPM by ALG3 is required for optimal DENV infection. In the ER lumen, the DPMS complex provides the mannose required for the synthesis of glycosylphosphatidylinositol anchor, the *N*-glycan precursor and the protein O-mannosylation (Fig. 5A). Each synthesis pathway possesses specific DPM-dependent mannosyltransferases that catalyze the transfer of mannose from DPM (Fig. 5A). For instance, ALG3 catalyzes the addition of the first dol-P-Man-derived mannose in an alpha-1,3 linkage to $Man_5GlcNAc_2$-PP-Do precursor (27). PIG-M and PIG-X are components of GPI mannosyltransferase 1, which catalyzes the transfer of the first mannose residue from DPM to a GlcN-(acyl)PI molecule (28). POMT1 and POMT2 initiate protein O-mannosylation by linking the initial mannose residue to the hydroxyl group of serine or threonine amino acids of nascent translocating proteins (29). To identify the DPM-dependent glycosylation pathway that is required for DENV infection, we ablated ALG3, POMT2, and PIG-M in HAP1 cells. In the case of ALG3 and POMT2, we generated single-cell clones (ALG3^{KO} and POMT2^{KO}). For PIG-M, we selected a CD59-deficient population by cell sorting (PIG-M^{KO}). Efficient gene deletion was validated by genomic DNA sequencing (Fig. 5B) and/or by monitoring the loss of surface expression of CD59 or the glycosylated α-dystroglycan (α-DG) receptors (Fig. 5C). In agreement with a previous study showing that cell surface expression of α-DG is reduced upon treatment with an N-glycosylation inhibitor (30), we observed a decrease of α-DG cell surface expression in ALG3^{KO} cells. We then challenged our KO cells with DENV at several MOIs. As shown in Fig. 5D, DENV infection was significantly reduced in ALG3^{KO} and DPM3^{KO} cells, while it was moderately or not affected in PIG-M^{KO} and POMT2^{KO} cells, respectively. Overall, we concluded that the absence of mannose addition to the N-glycan precursor in DPM^{KO} cells accounts for the major phenotype observed in DENV infection, although we could not exclude a marginal effect of blocking the GPI biosynthesis pathway.

DPMS is required for optimal DENV RNA replication. To determine which step of the viral life cycle requires DPMS complex activity, we first determined whether viral entry was impaired in DPM^{KO} cells. We challenged control, DPM3^{KO}, and DPM3-*trans*-complemented (DPM3^{KO}-DPM3) 293T cells with DENV2, trypsinized the cells at 4 h postinfection (hpi) to remove cell surface-bound particles, and quantified the levels of intracellular viral RNA (vRNA) by quantitative reverse transcription-PCR (RT-qPCR) as we previously described (31). The levels of internalized viral RNA in DPM3^{KO} and control cells were similar (Fig. 6A), suggesting that DENV entry was not impaired by DPM3 gene ablation. In contrast, at 24 hpi we observed a significant reduction of viral RNA in DPM3^{KO} cells compared to the levels in control and DPM3^{KO}-DPM3 cells, suggesting

FIG 1 Legend (Continued)
Genes of interest were colored according to their biological pathways. The *y* axis represents the significance of sgRNA enrichment of genes in the selected population compared to the unselected control population. The *x* axis represents a random distribution of the genes. (C) Sanger sequencing of *DPM1* and *DPM3* in control and DPM1 and DPM3 KO cells. PAM, protospacer adjacent motif. (D) Immunoblot of DPM1 in control, DPM1^{KO}, and DPM3^{KO} cells. (E) Cell surface CD59 staining on control and DPM1^{KO} or DPM3^{KO} HAP1 cells. (F) Control, DPM1^{KO}, and DPM3^{KO} HAP1 cells were plated and cell viability was assessed over a 72-h period using the CellTiter-Glo assay. (G and H) Control and DPM1 or -3 KO HAP1 cells were challenged with DENV2 JAM (MOIs of 2 and 20 in panel G and MOI of 5 in panel H). Levels of infection were quantified 48 hpi by flow cytometry using MAb 2H2 (G) or by immunofluorescence using MAb 2H2 or antibodies against NS3 (H). (I) Quantification of the viral particles released in the supernatant of inoculated HAP1 cells collected at 48 hpi. Virus titer was determined on Vero E6 cells by flow cytometry. FIU, flow cytometry infectious units. (C, D, E, F, and H) All data are representative of results from at least two independent experiments. (G and I) Data are means ± SD from three independent experiments performed in duplicate. Significance was calculated using a two-way ANOVA with Dunnett's multiple-comparison test. n.s, nonsignificant. ***, $P < 0.001$; ****, $P < 0.001$.

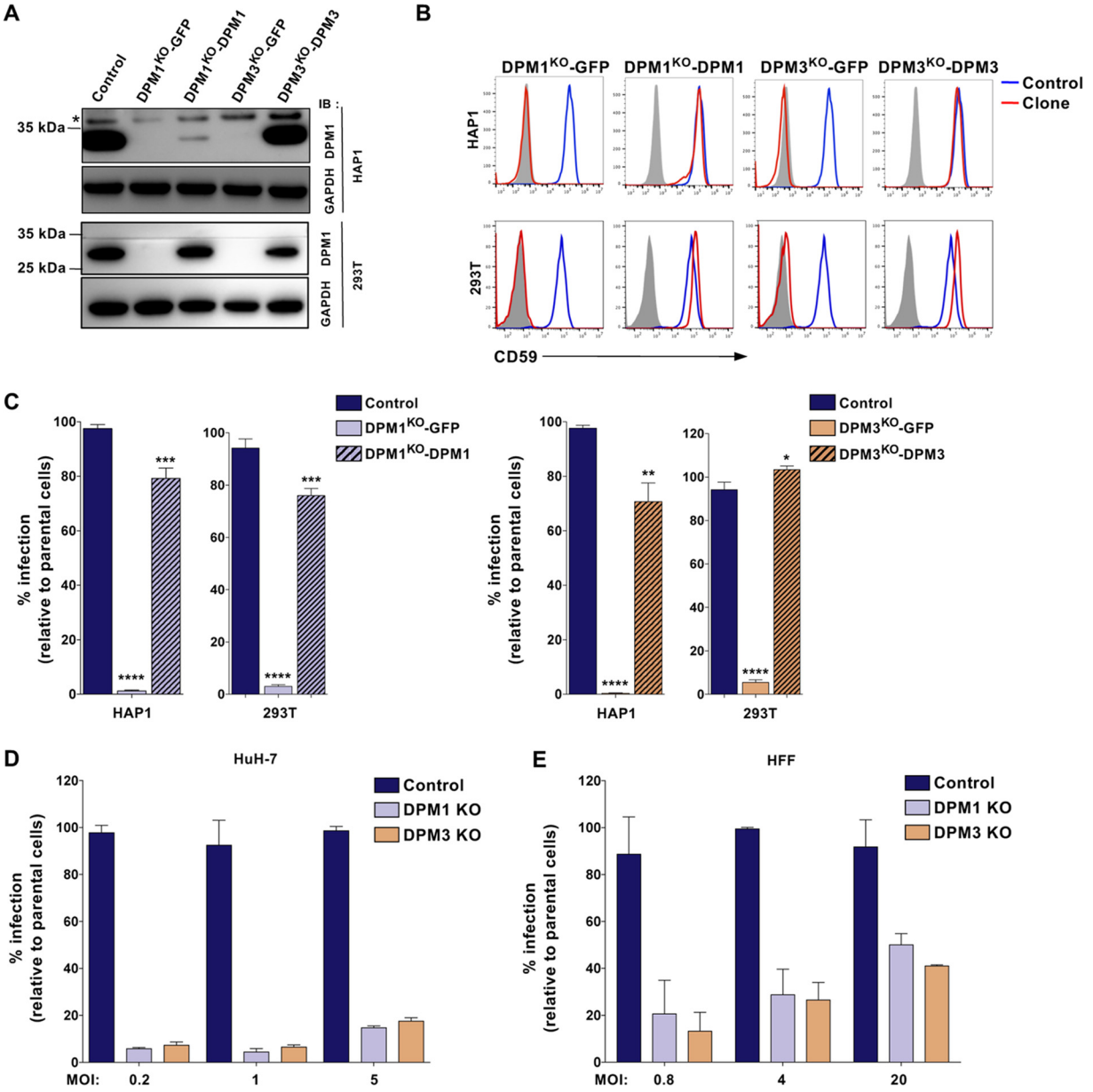

FIG 2 DPM1 and DPM3 *trans*-complementation restores cell susceptibility to DENV infection. (A) Immunoblot of DPM1 in control, DPM1^{KO}, and DPM3^{KO} cells *trans*-complemented with the respective cDNA. (B) Cell surface CD59 staining on 293T and HAP1 clones *trans*-complemented with DPM1 or DPM3 cDNA. (C) 293T and HAP1 *trans*-complemented clones were challenged with DENV2 JAM (MOI of 5 in 293T cells and MOI of 10 in HAP1 cells). Infection was quantified 48 hpi by flow cytometry using MAb 2H2. Data are means ± SD from three independent experiments performed in duplicate. Significance was calculated using a one-way ANOVA with Dunnett's multiple-comparison test. *, $P < 0.05$; **, $P < 0.01$; ***, $P < 0.001$; ****, $P < 0.001$. (D) Control and DPM1 and -3 KO Huh-7 clones were inoculated with increasing MOIs of DENV2 JAM. Levels of infection were quantified 48 hpi by flow cytometry using MAb 2H2. (E) HFF1 cells transfected with control, DPM1, or DPM3 sgRNA were inoculated with increasing MOIs of DENV2 JAM. Levels of infection were quantified 48 hpi by flow cytometry using MAb 2H2 in aCD59-negative population. (A, B, D, and E) Data are representative of results from at least two independent experiments.

that the DPMS complex acts on a postentry step of the DENV life cycle. Once delivered to the cytoplasm, the vRNA is translated, allowing the production of the viral nonstructural (NS) proteins, which, in turn, mediate the vRNA amplification. To assess the effect of the DPMS complex on DENV vRNA replication, we used the *Renilla* luciferase (Rluc) reporter subgenomic replicon sgDVR2A (32, 33). Control and DPM^{KO} 293T cells were transfected with *in vitro*-transcribed DVR2A subgenomic RNA and vRNA replication was monitored over time by quantifying the Rluc activity. As a positive control, we also transfected DVR2A subgenomic RNA in 293T knockout for STT3A, a subunit of the OST

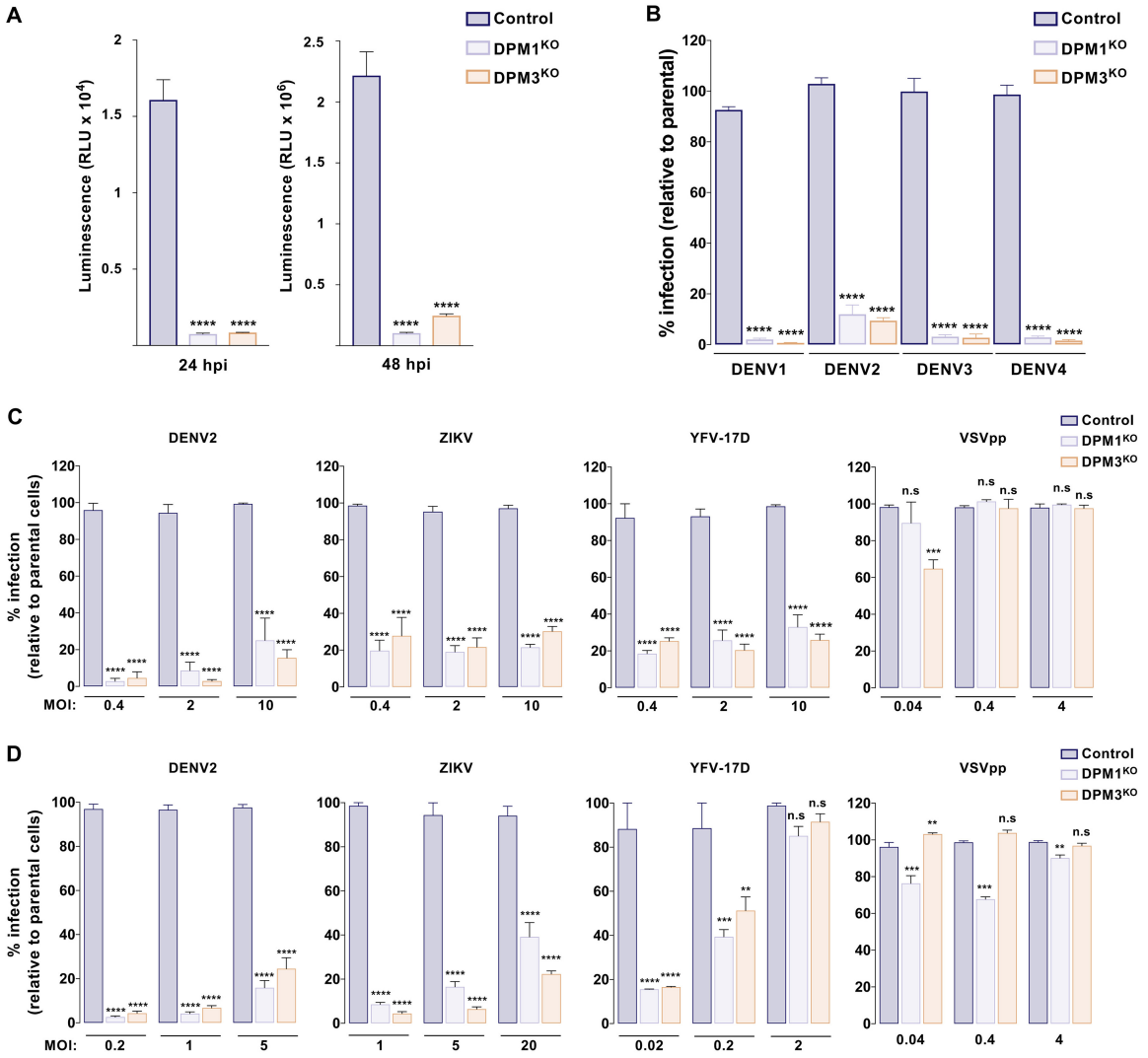

FIG 3 DPM1 and -3 are required by the four DENV serotypes and other related flaviruses. (A) Control, DPM1^{KO}, and DPM3^{KO} cells were inoculated with DENV2 16681 *Renilla* luciferase (Rluc) reporter virus (DVR2A; MOI of 0.5). At 24 and 48 hpi, Rluc activity was measured. RLU, relative light units. (B) Control, DPM1^{KO}, and DPM3^{KO} cells were inoculated with DENV1 KDH (MOI of 2), DENV2 NGC (MOI of 0.2), DENV3 THAI (MOI of 10), and DENV4 1086 (MOI of 0.2). Levels of infection were quantified 48 hpi by flow cytometry using MAb 2H2. Data are means ± SD from three independent experiments performed in duplicate. Significance was calculated using a one-way ANOVA with Tukey's multiple-comparison test. ****, $P < 0.0001$. (C and D) Control, DPM1^{KO}, and DPM3^{KO} HAP1 (C) and 293T (D) cells were inoculated with increasing MOIs of DENV2 16681, YFV 17D, ZIKV HD78788, or HIV pseudotyped with VSV-G envelope (VSVpp) expressing red fluorescent protein (RFP). Infection was quantified by flow cytometry 48 hpi by using MAb 4G2 (DENV and ZIKV) or 2D12 (YFV) or by monitoring RFP fluorescence. Data are means ± SD from two independent experiments performed in duplicate. Significance was calculated using a two-way ANOVA with Dunett's multiple-comparison test. **, $P < 0.01$; ***, $P < 0.001$; ****, $P < 0.0001$.

complex that plays a critical role in DENV RNA replication (10). We observed an increase of Rluc signal over time in WT cells and, to a lesser extent (10-fold reduction at 36 hpi), in DPM^{KO} cells. As expected, Rluc activity dropped over time in STT3A-deficient cells (Fig. 6B). Like other single-stranded RNA viruses, DENV produces double-stranded RNA (dsRNA) molecules as an intermediate during viral genome replication. To confirm that the DPMS complex is involved in viral genome replication, we sought to monitor the formation of dsRNA foci during infection in control, DPM1^{KO}, and DPM1^{KO}-complemented (DPM1^{KO}-DPM1) cells by immunofluorescence. Consistent with the kinetics of DENV replication showed in Fig. 6B, dsRNA foci appeared in control and DMP1^{KO}-DPM1 cells at 24 h after inoculation. Importantly, in DPM1-deficient cells we observed a 4.5-fold reduction in the number of foci (Fig. 6C). Together, these data showed that DPMS facilitates viral RNA production and/or accumulation after virus entry and uncoating, through a mechanism distinct from STT3A.

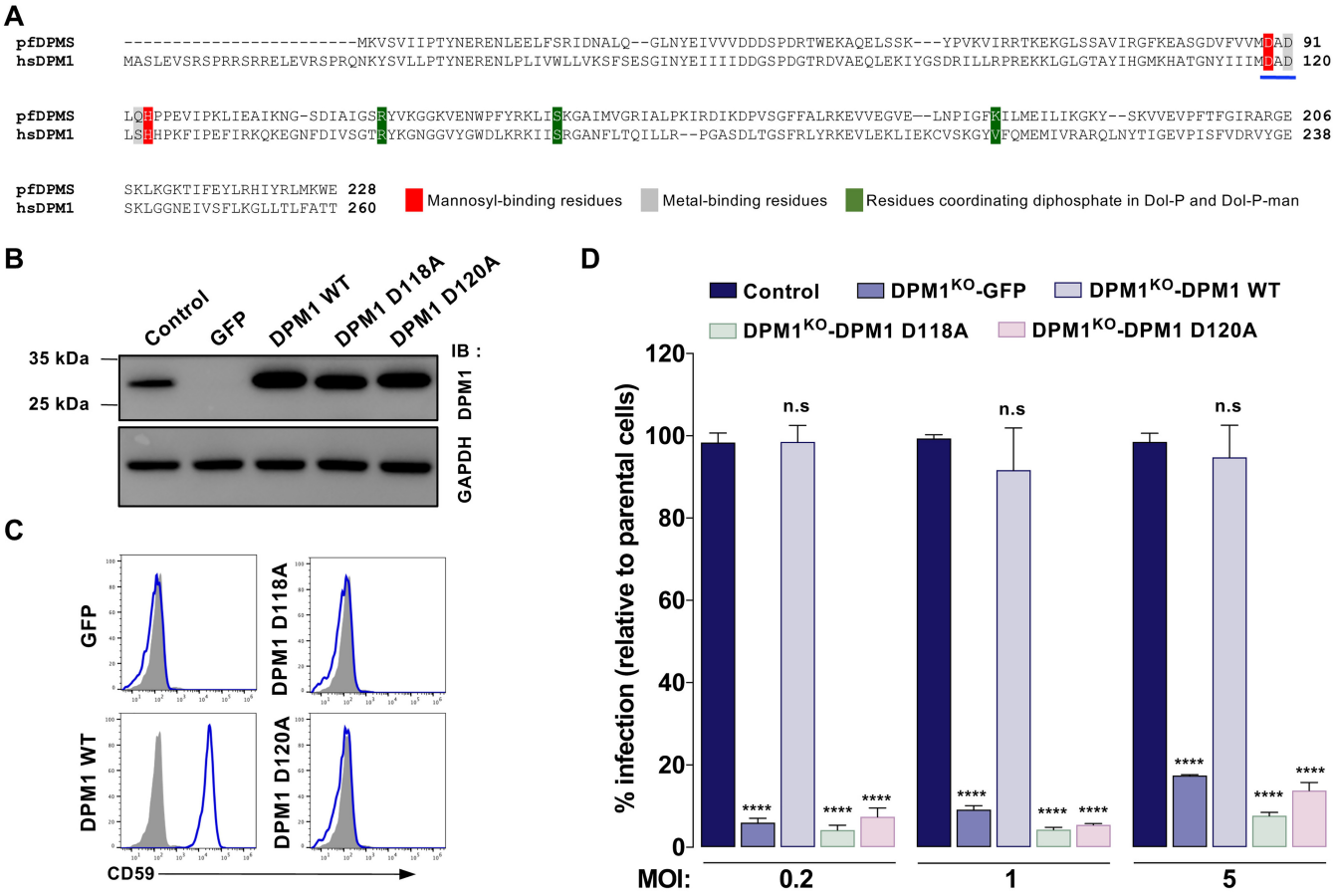

FIG 4 DENV infection requires DPM1 catalytic activity. (A) Sequence alignment of the catalytic domain of *Pyrococcus furiosus* DPMS (pfDPMS; UniProt accession number Q8U4M3) and *Homo sapiens* DPM1 (hsDPM1; UniProt accession number O60762). The DAD motif is underlined in blue. (B and C) Immunoblot analysis of DPM1 expression (B) and staining of cell surface CD59 (C) in DPM1^{KO} 293T cells complemented with the WT or DPM1 mutated in the catalytic site (D118A and D120A). Data are representative of reults from three independent experiments. (D) Control cells, DPM1^{KO} 293T cells, and DPM1^{KO} cells complemented with the WT or catalytically dead mutants of DPM1 were inoculated with increasing MOIs of DENV2 16681. Levels of infection were quantified 48 hpi by flow cytometry using MAb 2H2. Data are means ± SD from three independent experiments performed in duplicate. Significance was calculated using a two-way ANOVA with Dunett's multiple-comparison test. ****, $P < 0.0001$.

DPMS catalytic activity is important for viral protein glycosylation. DPM1 or AGL3 deficiency leads to the accumulation of $Man_5GlcNAc_2$-PP-Do in the ER lumen. This results in a peculiar N-glycosylation pattern because of the transfer of truncated oligosaccharides to proteins and/or the incomplete use of N-glycosylation sites (34–36). DENV encodes three glycosylated proteins: NS1, prM, and the E protein (37). A defect in glycosylation of these proteins has been shown to have dramatic consequences for DENV infection (37). Thus, we speculated that DPM1 ablation may affect the proper glycosylation of DENV proteins. To test this hypothesis, we assessed the migration profile of viral proteins by immunoblot analysis. 293T-DPM1^{KO} cells *trans*-complemented with either an empty vector, the WT, or the catalytically dead D118A and D120A DPM1 variants were transfected with cDNA encoding the C-prM-E precursor or the NS1 protein. Cells that received the C-prM-E plasmids were cotransfected with a plasmid encoding the DENV NS2B-NS3 viral protease necessary for the C protein cleavage. We found that when expressed in cells deficient for DPM1 catalytic activity and compared to the case with control cells, all the viral glycoproteins migrated at a lower molecular weight, likely representing abnormal glycosylation forms (Fig. 7A and B). Furthermore, we observed a decrease in the expression for prM and E proteins (Fig. 7A). In contrast, in cells complemented with DPM1 WT, all glycoproteins appeared at the correct size, and the expression of prM and E was partially restored. Previous results have indicated that $Man_5GlcNAc_2$ oligosaccharide is peptide-*N*-glycosidase F

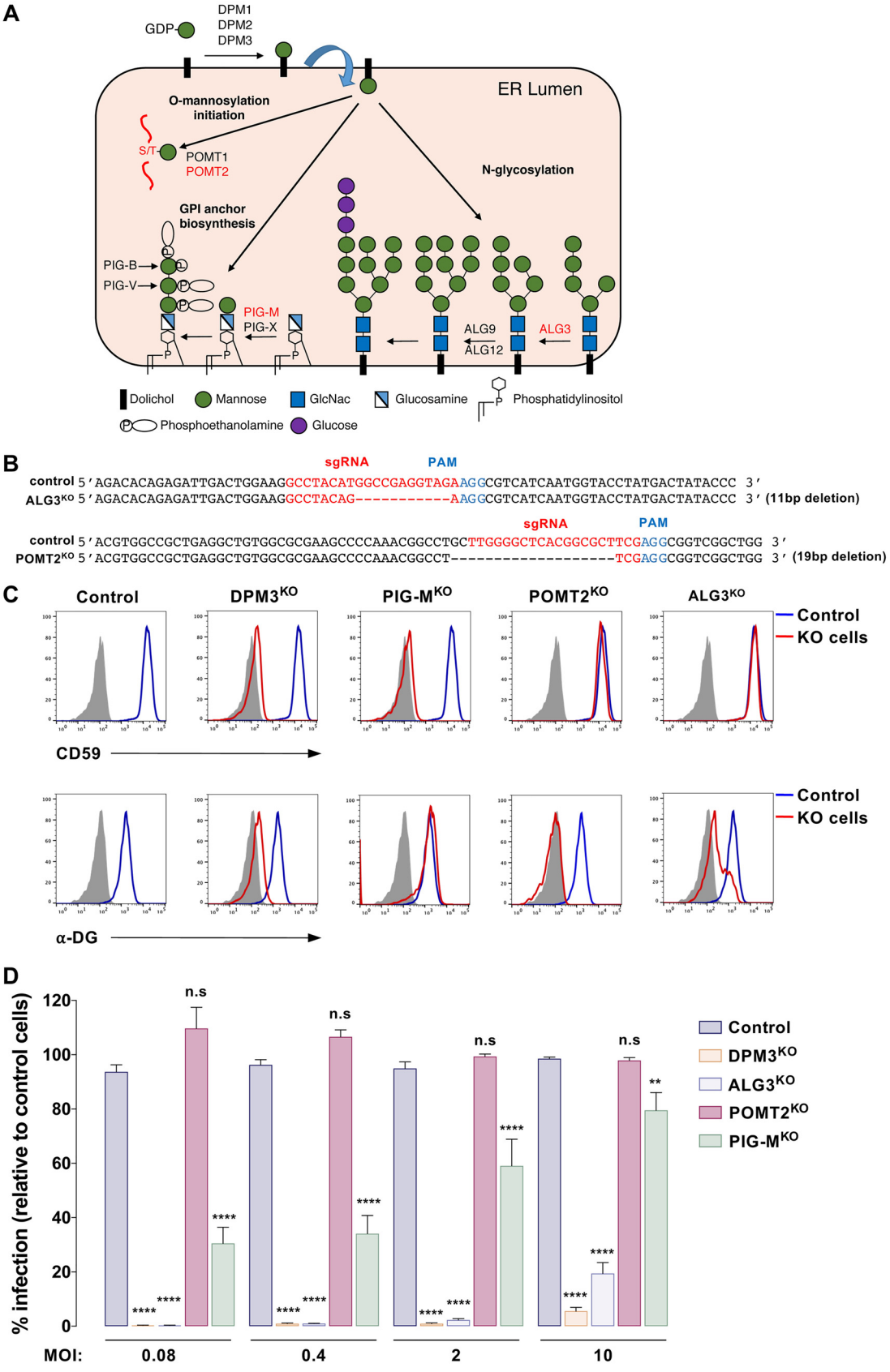

FIG 5 DENV infection requires transfer of mannose from DPM to lipid-linked oligosaccharide by ALG3 mannosyltransferase. (A) Schematic representation of the ER DPM-dependent pathways and their related mannosyltransferases. Mannosyltransferases

(Continued on next page)

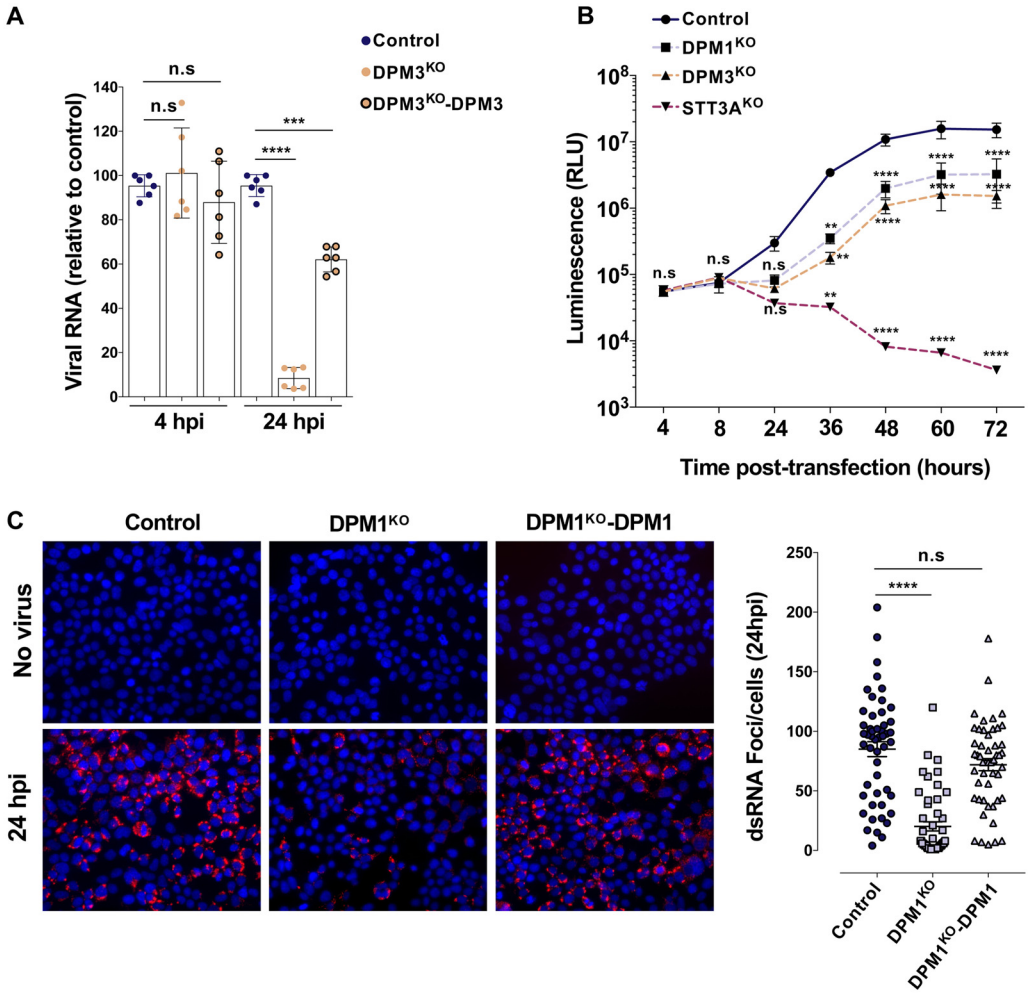

FIG 6 The DPMS complex is required for optimal viral RNA replication. (A) Control, DPM3^{KO}, and DPM3^{KO} 293T cells complemented with DPM3 were inoculated with DENV 11681 (MOI of 10). At 4 and 24 hpi, cells were treated with trypsin to remove cell surface-bound virus and viral RNA was quantified by RT-qPCR. Data are means ± SD from two independent experiments performed in triplicate. Significance was calculated using a one-way ANOVA with Tukey's multiple-comparison test. ***, $P < 0.001$; ****, $P < 0.0001$). (B) Control, DPM1^{KO}, DPM3^{KO}, and STT3A^{KO} 293T cells were transfected with *in vitro*-transcribed subgenomic DENV2 RNA expressing the *Renilla* luciferase. Rluc activity was monitored at the indicated time points. Data are means ± SD from two independent experiments performed in quadruplicate. Significance was calculated using a two-way ANOVA with Dunett's multiple-comparison test. **, $P < 0.01$; ****, $P < 0.0001$. (C) Control, DPM1^{KO}, and DPM1^{KO} 293T cells complemented with DPM1 were inoculated with DENV2 16681 (MOI of 100). Left, representative images of the cells stained with anti-dsRNA MAb J2 at 24 hpi. Right, quantification of the number of foci per cell using Icy software. Data are means ± SD from a representative experiment with $n = 50$ independent cells. Significance was calculated using a one-way ANOVA with Dunnett's multiple-comparison test. ****, $P < 0.0001$.

(PNGase F) sensitive and endo-β-*N*-acetylglucosaminidase H (endo H) resistant. To ascertain whether the abnormal glycoprotein N-glycosylation seen in DPM1^{KO} cells resulted from the transfer of truncated $Man_5GlcNAc_2$ oligosaccharides, we treated our cell lysates with PNGase F or endo H prior to immunoblot analysis. As shown in Fig. 7C, in control cells, the viral proteins were sensitive to both PNGase F and endo H, whereas

FIG 5 Legend (Continued)
invalidated in this study are depicted in red. (B) Sanger sequencing of ALG3 and POMT2 in control and ALG3^{KO} or POMT2^{KO} HAP1 clones. (C) Cell surface staining of CD59 and glycosylated α-dystoglycan on HAP1 cells deficient for DPM3, PIG-M, and POMT2. The blue line represents staining with the respective Ab and gray shading staining with the matching isotypes in control cells. Data are representative of results from three independent experiments. (D) Control and HAP1 cells with KO of the indicated genes were inoculated with increasing MOIs of DENV2 11681, and levels of infection were quantified 48 hpi by flow cytometry using MAb 2H2. Data are means ± SD from three independent experiments performed in duplicate. Significance was calculated using a two-way ANOVA with Dunett's multiple-comparison test. *, $P < 0.05$; **, $P < 0.01$; ***, $P < 0.001$; ****, $P < 0.0001$.

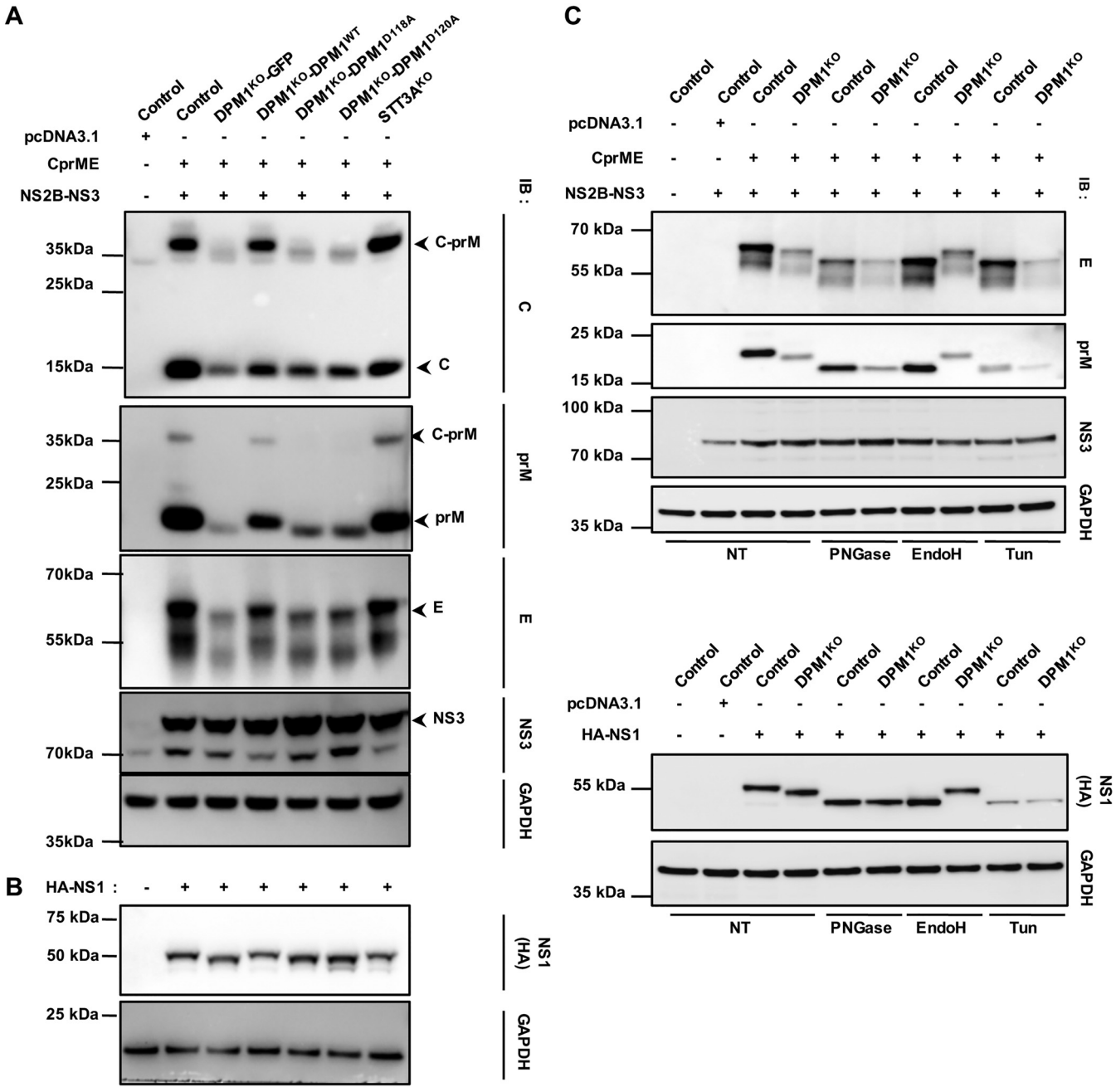

FIG 7 Effect of DPM1 depletion on DENV viral protein glycosylation. Control, DPM1^{KO}, and STT3A^{KO} 293T cells and DPM1^{KO} cells complemented with the WT or catalytically dead mutants of DPM1 were cotransfected with DENV C-prM-E and NS2B-NS3 plasmids (1:1 ratio) (A) or transfected with DENV hemagglutinin (HA)-tagged NS1 plasmid (B). Cell lysates were subjected to immunoblot analysis with anti-capsid, anti-prM, anti-E, and anti-HA antibodies. Data are representative of results from three independent experiments. (C) Control and DPM1^{KO} 293T cells were cotransfected with DENV C-prM-E and NS2B-NS3 plasmids or HA-NS1 plasmid. Twenty micrograms of total proteins was subjected to deglycosylation with either PNGase F or endo H (25 kU ml^{-1}) for 1 h at 37°C and analyzed by immunoblotting with anti-prM, anti-E, and anti-HA antibodies. As a positive control for deglycosylation, cells were also transfected in the continuous presence of tunicamycin (Tun; 5 μg ml^{-1}). For all panels, blots are representative of those from three independent experiments. NT, nontreated.

in DPM1^{KO} cells, N-glycans were sensitive only to PNGase F, suggesting that truncated oligosaccharides were transferred to viral proteins. Taken together, these data indicate that a deficiency in DPMS activity impairs the correct glycosylation of DENV proteins and thus ultimately inhibits infection.

DENV envelope glycoprotein epitope accessibility is altered in DPM1-deficient cells. In the ER, the N-glycosylation pathway contributes to glycoprotein folding (38). In addition, several studies have reported that mutations of N-glycan sites have an

adverse effect on viral glycoprotein folding (39–41). To investigate whether DENV glycoproteins were properly folded in DPM1^{KO} cells, we transfected control and DPM1^{KO} 293T cells with a plasmid encoding C-prM-E and then performed an immunoprecipitation (IP) assay with monoclonal antibody (MAb) 2H2 or 4G2. These antibodies recognize conformational epitopes in prM and E protein, respectively, and are sensitive to correct protein folding (42, 43). A similar approach was previously used to investigate the proper folding of truncated E protein expressed with prM in the S2 cell system (44). Although similar amounts of viral glycoproteins were subjected to immunoprecipitation, the quantity of the E protein immunoprecipitated with MAb 4G2 from DPM1^{KO} cells was decreased by 75% compared to the quantities in control and STT3A^{KO} cells (Fig. 8A). These results suggest that E glycoprotein is potentially misfolded in DPM1-depleted cells. Expression of prM in DPM1^{KO} cells led to an increase of the immunoreactivity with MAb 2H2 compared to the case with control cells (Fig. 8B). This is in agreement with N-glycosylation contribution to immune evasion by glycan shielding of viral particles and modulation of immunogenicity (45–48). In contrast, NS1 is similarly immunoprecipitated in DPM1/3-depleted cells and control cells (Fig. 8C). Overall, the alterations of immunoreactivity observed with conformational antibodies suggest that the transfer of truncated $Man_5GlcNAc_2$ oligosaccharide in DPM1-deficient cells affected the exposure of structural viral glycoprotein epitopes.

Conclusions and perspectives. In this study, we performed a genome-wide CRISPR-Cas9 screen in haploid HAP1 cells and identified host genes required for DENV infection. Our work highlights an important role for the DPM1 and -3 proteins in efficient DENV infection. To our knowledge, this is the first study describing and characterizing DPM1 and -3 as virus host dependency factors. Interestingly, the DPM3 gene was recently identified as a gene candidate in a recent ZIKV CRISPR-Cas9 screen (11). It is puzzling that DPM1 and -3 were not identified in the recent DENV genome-wide CRISPR-Cas9 screens that used the same sgRNA libraries. Given that these screens were performed with 293T and Huh7.5.1 cells, it is conceivable that sgRNAs targeting DPM1 and -3 provide a less effective selective advantage in these cells than in HAP1 haploid cells. This speculation is supported by the identification of DPM3 as a candidate for ZIKV infection in a haploid CRISPR-Cas9 screen but not in four independent screens done in Huh7.5.1 cells infected with the DENV1 to -4 serotypes (11). Surprisingly, DENV screening of a HAP1 cell library with knockout mutations, generated by insertional mutagenesis, did not identify DPM1 or DPM3 as a DENV host factor (10). Nonetheless, this screen also failed to identify SEC61A1 or other translocon subunits which were identified in our screen and other flavivirus CRISPR-Cas9 screens (9, 10, 19).

We provide evidence that DPMS is required for both efficient viral RNA amplification and the proper glycosylation of the viral proteins NS1, prM, and E. The effect of DPM depletion on viral replication may result from the incorrect glycosylation of NS1, a protein essential for the formation of the replication complex (49). This hypothesis is consistent with the previous observation that DENV mutants lacking N-glycan on NS1, which contains two glycosylation sites (at Asn130 and Asn207), failed to replicate efficiently in human cells (50). Mutation of the N207 site in DENV2 led to reduced virus growth in C6/36 cells and attenuated mouse neurovirulence (51). Similarly, mutation of the N130 site affects DENV1 growth (52). Interestingly, ablation of all glycosylation sites in WNV NS1 led to perinuclear localization of the protein (53). This correlates with malformed virus-induced vesicles that likely hamper viral replication and results in virus attenuation. This phenotype was also reported for DENV NS1 glycosylation mutants (51) and is consistent with our observation of reduced dsRNA focus formation in DPM3 KO cells. In line with the role of NS1 glycosylation in virus replication, our work complements our previous study showing that NGI, a small inhibitor of the OST complex, strongly impairs NS1 glycosylation and blocks DENV infection (54).

In DPM1-deficient cells, transfer of truncated oligosaccharides to viral glycoproteins affects prM and E protein folding. Furthermore, we observed that in DPM1^{KO} cells, prM and E proteins were reproducibly less expressed. One can speculate that the incorpo-

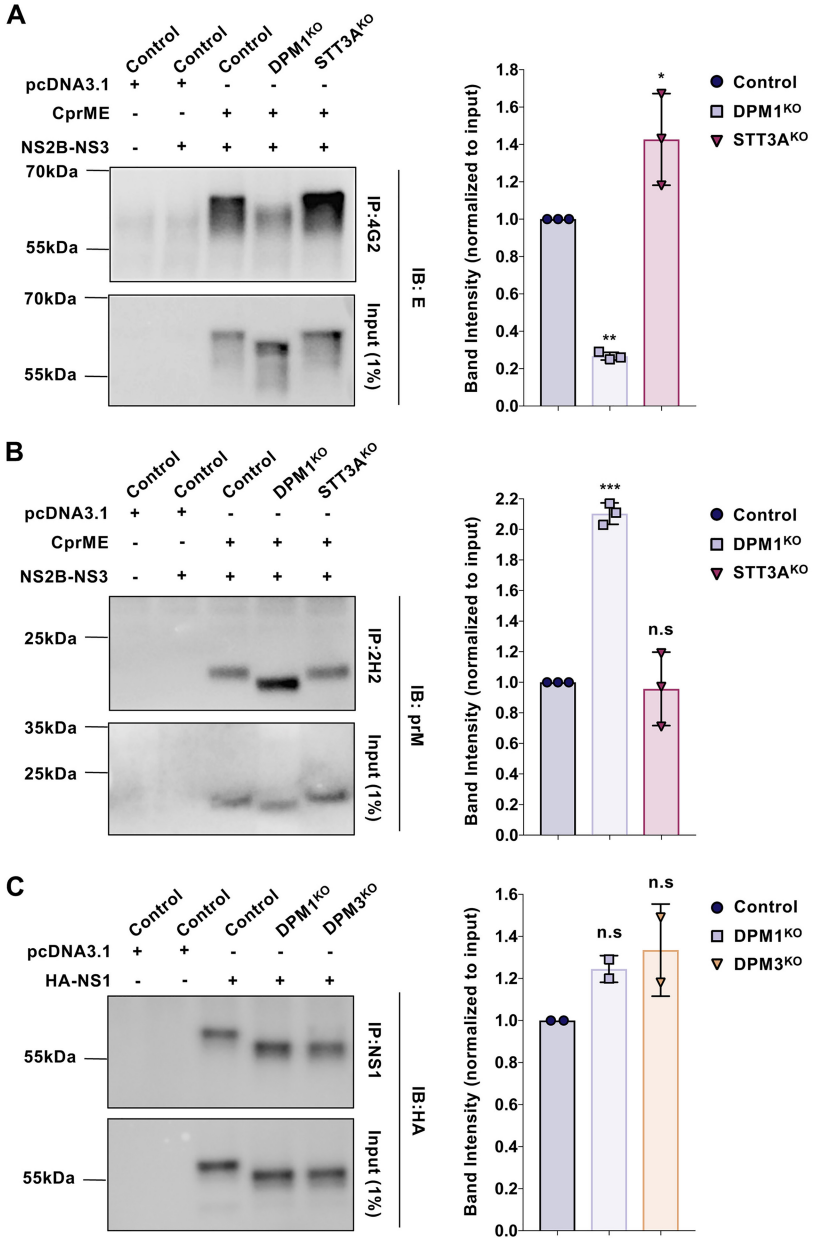

FIG 8 DPM1 deficiency affects E and prM glycoprotein epitope accessibility. Control, DPM1^{KO}, and STT3A^{KO} 293T cells were cotransfected with DENV C-prM-E and NS2B-NS3 plasmids (1:1 ratio). (A) Relatively equivalent amounts of viral glycoproteins were immunoprecipitated with MAb 4G2, followed by immunoblot analysis with anti-E antibodies. (B) Relatively equivalent amounts of viral glycoproteins were immunoprecipitated with MAb 2H2, followed by immunoblot analysis with anti-prM antibodies. (C) Control, DPM1^{KO}, and DPM3^{KO} 293T cells were transfected with DENV HA-NS1 plasmid. Relatively equivalent amounts of viral glycoproteins were immunoprecipitated with commercially available (Abcam; ab41623) anti-NS1, followed by immunoblot analysis with anti-HA antibody. Blots are representative of those from three independent experiments. Bar graphs represent quantification of the chemiluminescent band intensities relative to E, prM, and NS1 expression in control cells. Each point plotted corresponds to the quantification from one transfection experiment. Data are means ± SD from from three (A and B) or two (C) independent transfection experiments. Significance was calculated using a one-way ANOVA with Dunnett's multiple-comparison test. *, $P < 0.05$; **, $P < 0.01$; ***, $P < 0.001$.

ration of truncated oligosaccharides decreases the glycoprotein stability. Interestingly, proteins directed for degradation by the ER-associated degradation (ERAD) pathway possess $Man_5GlcNAc_2$ or $Man_6GlcNAc_2$ glycoforms (55). This leads to the trimming of mannose residues from nascent proteins that do not reach a completely folded

conformation in order to facilitate their dislocation and removal from the calnexin/calreticulin (CNX/CRT) folding cycle. This extensive demannosylation by ER mannosidases generates $Man_5GlcNAc_2$ or $Man_6GlcNAc_2$ oligosaccharides, which are recognized by the two ERAD lectin receptors, OS-9 and XTP3-B, responsible for delivery of unfolded proteins to the ERAD pathway (56). Given that the CNX/CRT chaperones recognize $Glc_1Man_9GlcNAc_2$ on proteins to initiate the folding cycle, one can speculate that truncated $Man_5GlcNAc_2$ oligosaccharides may restrict the entry of the prM and E glycoproteins in the CNX/CRT folding cycle, leading to protein misfolding. Simultaneously, OS-9 and XTP3-B, which have high affinity for $Man_5GlcNAc_2$ glycoforms, may enhance the delivery of nascent glycoproteins to the ERAD pathway by bypassing the requirement for mannose trimming. Thus, structural glycoproteins misfolding and degradation likely impede virus particle release and viral dissemination, which is consistent with previous studies showing the adverse effect of mutations of N-glycan sites on the release of flavivirus virions (57–59).

MATERIALS AND METHODS

Cell lines. HEK293FT cells, HFF1 human foreskin fibroblasts (gift from D. Missé, MIVEGEC, Montpellier, France), Huh7.5.1 cells, and Vero cells were maintained in Dulbecco modified Eagle medium (DMEM; Thermo Fisher Scientific) with 10% fetal bovine serum (FBS), 1% penicillin-streptomycin, and 2 mM L-glutamine (Life Technologies). HAP1 cells were purchased from Horizon Discovery and cultured according to the manufacturer's instructions.

Virus strains. DENV1 KDH0026A (gift from L. Lambrechts, Pasteur Institute, Paris), DENV2 JAM (Jamaica), DENV2 New Guinea C (NGC), DENV2 Thaïland/16681/84 (16681), DENV3 Thailand (THAI), DENV4 1086, ZIKV HD78788, and YFV 17D were propagated and titers were determined as previously described (60). The DENV2 Rluc reporter virus (DVR2A) was produced as previously described (33), and infection was determined by measuring the Rluc activity using a TriStar² LB942 microplate reader (Berthold Technologies). Red fluorescent protein (RFP)-expressing lentiviral vectors pseudotyped with vesicular stomatitis virus glycoprotein G (VSV-G) were generated by transfecting HEK293FT cells with pNL4.3 Luc RFP ΔEnv, psPAX2, and pVSV-G (4:3:1 ratio) using Lipofectamine 3000. Supernatants were harvested 48 h after transfection, cleared by centrifugation, and filtered, and then aliquots were frozen at −80°C.

Antibodies and reagents. All antibodies and reagents are listed in Table 1.

Pooled CRIPSR screen and plasmid constructs. The GeCKO v2 human CRISPR pooled libraries (A and B) encompassing 123,411 different sgRNAs targeting 19,050 genes were purchased from GenScript. Genome-wide CRISPR-Cas9-edited HAP1 cells were generated as previously described (61). Sixty million cells from each library were independently infected with the primary strain DENV2 JAM using an MOI of 5, and cells that survived the cytopathic effect were collected 2 weeks later. Genomic DNA was extracted from selected cells or the corresponding uninfected library cells using a QIAamp DNA column (Qiagen), and inserted gRNA sequences were amplified and sequenced using next-generation sequencing on an Illumina Miseq (Plateforme MGX, Institut Génomique Fonctionelle, Montpellier, France). sgRNA sequences were analyzed using MAGeCK software.

Gene editing and *trans*-complementation experiments. sgRNAs targeting DPM1, DPM3, STT3A, ALG3, PIG-M, and POMT2 were designed using CRISPOR software (http://crispor.org). Sequences for all the sgRNAs are listed in Table 1. The sgRNAs were cloned into plasmid lentiCRISPR v2 (Addgene) according to the recommendations of members of the Zhang laboratory. HAP1 and HEK293FT gene-edited cells were generated as previously described (61).

The human DPM1 and -3 open reading frames (ORF) were amplified by RT-PCR from RNA extracted from HAP1 cells. Amplification products were cloned into an XhoI-BamHI (DPM1)- or EcoRI-BamHI (DPM3)-digested pLVX-IRES-ZsGreen1 vector. Catalytic-site DPM1 mutants were generated using QuikChange site-directed mutagenesis (Agilent) performed following the manufacturer's instructions. All primers are listed in Table 1.

Flow cytometry analysis. Flow cytometry analysis was performed as previously described (62). For cell surface staining, cells were incubated with mouse anti-human CD59 (Novus Biologicals) or mouse anti-human N-glycosylated α-dystroglycan (Santa Cruz; 5 μg ml^{-1}). DENV infection was detected using anti-prM MAb 2H2, ZIKV infection was detected using anti-E MAb 4G2, and YFV infection was detected using anti-E MAb 2D12. Acquisition was performed on an Attune NxT flow cytometer with Attune NxT software (Thermo Fisher Scientific), and data were analyzed using FlowJo software (Tree Star, Olten, Switzerland).

Infectious virus yield assay. To assess the release of infectious particles during infection, cells were inoculated for 3 h, washed once, and then maintained in the culture medium over a 72-h period. At the desired time points, supernatants were collected and kept at −80°C. Vero E6 cells were incubated with 3-fold serial dilutions of supernatant for 24 h, and prM expression was quantified by flow cytometry as described above.

Immunofluorescence assay. Control and knockout cells were cultured on Lab-Tek II CC² chamber slides (Nunc, Roskilde, Denmark) for 24 h. Cells were inoculated with DENV2 JAM (MOI of 5) for 48 h and then washed twice with cold phosphate-buffered saline (PBS), fixed with 4% (vol/vol) paraformaldehyde

TABLE 1 Key resources[a]

Reagent or resource	Source or sequence	Identifier
Antibodies		
Mouse anti-DPM1 (A-5)	Santa Cruz Biotechnology	sc-515721
Mouse anti-GAPDH (0411)	Santa Cruz Biotechnology	sc-47724
Rabbit anti-dengue virus envelope protein antibody	GeneTex	GTX127277
Rabbit anti-dengue virus prM protein antibody	GeneTex	GTX128093
HA tag rabbit MAb	Cell Signaling Technology	3724
Polyclonal rabbit anti-mouse immunoglobulins/HRP	Agilent Technologies	P0260
Peroxidase AffiniPure donkey anti-rabbit IgG (H+L)	Jackson ImmunoResearch	711-035-152
Mouse IgG2A isotype control (clone 20102)	R&D Systems	MAB003
CD-59 antibody (MEM-43)	Novus Biologicals	NB500-330
Mouse anti-α-dystroglycan IIHC4	Santa Cruz Biotechnology	sc-73586
Alexa Fluor 647 AffiniPure donkey anti-mouse IgG (H+L)	Jackson ImmunoResearch	715-605-150
Alexa Fluor 488 AffiniPure goat anti-mouse IgG (H+L)	Jackson ImmunoResearch	115-545-003
FITC AffiniPure F(ab')$_2$ fragment goat anti-mouse IgG + IgM (H+L)	Jackson ImmunoResearch	115-096-068
Mouse anti-dengue virus NS3 protein antibody (GT2811)	GeneTex	GTX629477
Anti-dengue virus NS1 glycoprotein antibody (DN2)	Abcam	Ab41623
Chemicals and reagents		
PNGase F	New England BioLabs	P0704S
Endo H	New England BioLabs	P0702S
gRNA for CRISPR/Cas9 KO		
Control	GAGCTGGACGGCGACGTAAA	
DPM1	TTAGGAACTGCATATATTCA	
DPM3	GTCCGCCGGCTGCTATGCCC	
PIGM	CCGCGCGCTTCGTCACGGAG	
POMT2	TTGGGGCTCACGGCGCTTCG	
ALG3	GCCTACATGGCCGAGGTAGA	
STT3A	GCGATTGTCCTATGAGAAGC	
DPM1 mutants primers for site-directed mutagenesis		
DPM1 Forward	ATAAGAATGCGGCCGCGCCATGGCCTCCTTGGAAGTCAGTCGTAGTCC	
DPM1 Reverse	CGCGGATCCGCGTCATGTAGTAGCAAAAAGAGTCAATAATCCTTTC	
DPM3 Forward	CCGGAATTCCGGATGtacccatacgatgttccagattacgctACGAAATTAGCGCAGTGGC	
DPM3 Reverse	CGCGGATCCGCGTCAGAAGCGCAGCCCCCTGCGGGC	
DPM1 D118A Forward	GAAACTACATCATTATTATGGCTGCTGATCTCTCACACCATCC	
DPM1 D118A Reverse	GGATGGTGTGAGAGATCAGCAGCCATAATAATGATGTAGTTTC	
DPM1 D120A Forward	CTACATCATTATTATGGATGCTGCTCTCTCACACCATCCAAAATTTA	
DPM1 D120A Reverse	TAAATTTTGGATGGTGTGAGAGAGCAGCATCCATAATAATGATGTAG	
qPCR primers		
DENV2 JAM Env-F	TTCTCACTTGGAATGCTGCAA	
DENV2 JAM Env-R	GCCACAAGGGCCATGAAC	
Hs_GAPDH_2_SG QuantiTect primer assay	Qiagen	QT01192646

[a]Restriction endonuclease sites are underlined. Lowercase sequences correspond to HA tag coding sequences. HRP, horseradish peroxidase; FITC, fluorescein isothiocyanate.

(PFA) diluted in PBS for 20 min at room temperature, and permeabilized with 0.5% Triton X-100 in PBS-bovine serum albumin (BSA; 3%). DENV antigens were stained with the anti-prM MAb 2H2 or with anti-NS3 MAb. For dsRNA staining, cells were inoculated with DENV2 16681 (MOI of 100) for 24 h and then stained with the anti-dsRNA MAb J2. Antibodies were diluted (5 μg ml^{-1}) in PBS supplemented with 3% (wt/vol) BSA and 0.1% Triton X-100. Slides were mounted with ProLong gold antifade reagent containing 4′,6-diamidino-2-phenylindole (DAPI) for nucleus staining (Thermo Fisher Scientific).

Immunoprecipitation and immunoblotting. For immunoprecipitation (IP) analysis of prM and E proteins, transfected cells were lysed in Pierce IP lysis buffer (Thermo Scientific) in the presence of Halt protease inhibitor cocktail (Thermo Scientific) for 30 min at 4°C. The relative amount of prM or E protein in the lysate was determined by immunoblotting, and then equivalent amounts of viral proteins were incubated with either 5 μg of anti-prM 2H2 or anti-E 4G2 conformational MAb or with a 1/50 dilution of anti-NS1 overnight at 4°C, followed by incubation with protein G magnetic beads for 3 h. The beads were washed three times with BO15 and resuspended in LDS sample buffer (4×; Thermo Fisher Scientific) containing 25 mM dithiothreitol (DTT). Proteins were eluted by heating 5 min at 95°C and next were separated by SDS-PAGE. Immunoblotting was performed as previously described (61) with anti-E and anti-prM rabbit polyclonal antibodies (GeneTex).

PNGase F and endo H digestion. Lysates were subjected to PNGase F or endo H (New England BioLabs) digestion following the manufacturer's guidelines. Briefly, transfected cells were lysed as described above. A total of 20 μg of proteins, determined by DC protein assay (Bio-Rad), was diluted in water (2 mg ml^{-1} final concentration) and denatured for 10 min at 100°C. Prior to PNGase F digestion, Nonidet P-40 substitute (NP-40) was added at a final concentration of 1% vol/vol. PNGase F and endo H were added at a concentration of 25,000 U ml^{-1}, and the solutions were incubated for 1 h at 37°C. Completion of the digestion was confirmed by immunoblotting.

RNA purification, cDNA synthesis, and real-time qPCR. The experiment was performed as previously described (61). Briefly, control and DPM3^{KO} 293T cells were plated on 60-mm dishes (400,000 cells) and inoculated with DENV2 16681 (MOI of 10). At the desired time points, cells were incubated with 0.25% trypsin for 5 min at 37°C to remove cell surface-bound particles, and total RNA was extracted using the RNeasy Plus minikit (Qiagen) according to the manufacturer's instructions. cDNAs were generated from 500 ng of total RNA using the Maxima first-strand synthesis kit (Thermo Fisher Scientific). RT-qPCR was performed using a Power Syber green PCR master mix (Thermo Fisher Scientific) on a Light Cycler 480 (Roche). The primers used for RT-qPCR were as follows: for DENV2, forward primer 5′-TTCTCACTTG GAATGCTGCAA-3 and reverse primer 5′-GCCACAAGGGCCATGAAC-3′) for viral RNA quantification; for glyceraldehyde-3-phosphate dehydrogenase (GAPDH), Quantitect primers (purchased from Qiagen). Quantification using relative expression was performed based on the comparative threshold cycle (C_T) method, using GAPDH as an endogenous reference control.

Cell viability assay. Cell viability and proliferation were assessed over a 72-h period using the CellTiter-Glo 2.0 assay (Promega) as previously described (61).

Statistical analyses. Graphical representation and statistical analyses were performed using Prism7 software (GraphPad Software). Unless otherwise stated, the results are expressed as means ± standard deviations (SD) from three independent experiments performed in duplicate. Differences were tested for statistical significance using an unpaired two-tailed *t* test or one-way or two-way analysis of variance (ANOVA) with multiple comparisons with a *post hoc* test.

SUPPLEMENTAL MATERIAL

Supplemental material is available online only.

SUPPLEMENTAL FILE 1, XLSX file, 1.7 MB.

ACKNOWLEDGMENTS

Work in A.A.'s lab has received funding from the French Government's Investissement d'Avenir program, Laboratoire d'Excellence Integrative Biology of Emerging Infectious Diseases (grant ANR-10-LABX-62-IBEID), the Investissements d'Avenir program (ANR-10-IHUB-0002), ZIKAHOST (ANR-15-CE15-00029), and INSERM. E.S.-L. received funding from the ANR INCEPTION program (Investissements d'Avenir grant ANR-16-CONV-0005). A.L. is supported by a scholarship from the French Ministry of Research.

We thank Ralf Bartenschlager (Heidelberg, Germany) for providing us with the DENV *Renilla* luciferase reporter virus (DVR2A). We thank Louis Lambrechts for the DENV1 KDH0026A strain. We thank Dorothée Missé for providing us the human foreskin fibroblasts (HFF1) and the Genomic Platform (Gustave Roussy Cancer Campus) facility for sequencing.

L.M. and A.A. conceived the study. A.L., M.-L.H., L.B.-M., S.T., M.-L.C., C.D., A.A., and L.M. designed the experiments. L.M. performed the CRISPR-Cas9 screening and infection studies with A.L., M.-L.H., L.B.-M., and S.T. M.-L.H. generated *in vitro*-transcribed viral and RNA transfection experiments with L.M. A.L. performed the immunoprecipitation and Western blot studies with the help of M.-L.H. A.L. and L.M. validated the DPM1 and

3 gRNA and generated the DPM1 and DPM3 knockout cells described in this study. A.L. performed the immunofluorescence microscopy experiments and quantification. A.L. and L.M. performed the qPCR experiment. L.M. and E.S.-L. analyzed the gRNA sequencing and identified the hits. L.M. and A.A. wrote the initial manuscript draft, and the other authors contributed to editing into its final form.

REFERENCES

1. Holbrook MR, Holbrook M. 2017. Historical perspectives on flavivirus research. Viruses 9:97. https://doi.org/10.3390/v9050097.
2. Halstead SB. 2007. Dengue. Lancet 370:1644–1652. https://doi.org/10.1016/S0140-6736(07)61687-0.
3. Brady OJ, Gething PW, Bhatt S, Messina JP, Brownstein JS, Hoen AG, Moyes CL, Farlow AW, Scott TW, Hay SI. 2012. Refining the global spatial limits of dengue virus transmission by evidence-based consensus. PLoS Negl Trop Dis 6:e1760. https://doi.org/10.1371/journal.pntd.0001760.
4. Bhatt S, Gething PW, Brady OJ, Messina JP, Farlow AW, Moyes CL, Drake JM, Brownstein JS, Hoen AG, Sankoh O, Myers MF, George DB, Jaenisch T, Wint GR, Simmons CP, Scott TW, Farrar JJ, Hay SI. 2013. The global distribution and burden of dengue. Nature 496:504–507. https://doi.org/10.1038/nature12060.
5. Hadinegoro SR, Arredondo-Garcia JL, Capeding MR, Deseda C, Chotpitayasunondh T, Dietze R, Muhammad Ismail HI, Reynales H, Limkittikul K, Rivera-Medina DM, Tran HN, Bouckenooghe A, Chansinghakul D, Cortes M, Fanouillere K, Forrat R, Frago C, Gailhardou S, Jackson N, Noriega F, Plennevaux E, Wartel TA, Zambrano B, Saville M, CYD-TDV Dengue Vaccine Working Group. 2015. Efficacy and long-term safety of a dengue vaccine in regions of endemic disease. N Engl J Med 373:1195–1206. https://doi.org/10.1056/NEJMoa1506223.
6. Ferguson NM, Rodriguez-Barraquer I, Dorigatti I, Mier Y-R, Laydon DJ, Cummings DA. 2016. Benefits and risks of the Sanofi-Pasteur dengue vaccine: modeling optimal deployment. Science 353:1033–1036. https://doi.org/10.1126/science.aaf9590.
7. Acosta EG, Kumar A, Bartenschlager R. 2014. Revisiting dengue virus-host cell interaction: new insights into molecular and cellular virology. Adv Virus Res 88:1–109. https://doi.org/10.1016/B978-0-12-800098-4.00001-5.
8. Zeidler JD, Fernandes-Siqueira LO, Barbosa GM, Da Poian AT, Zeidler J, Fernandes-Siqueira L, Barbosa G, Da Poian A. 2017. Non-canonical roles of dengue virus non-structural proteins. Viruses 9:42. https://doi.org/10.3390/v9030042.
9. Lin DL, Cherepanova NA, Bozzacco L, MacDonald MR, Gilmore R, Tai AW. 2017. Dengue virus hijacks a noncanonical oxidoreductase function of a cellular oligosaccharyltransferase complex. mBio 8:e00939-17. https://doi.org/10.1128/mBio.00939-17.
10. Marceau CD, Puschnik AS, Majzoub K, Ooi YS, Brewer SM, Fuchs G, Swaminathan K, Mata MA, Elias JE, Sarnow P, Carette JE. 2016. Genetic dissection of Flaviviridae host factors through genome-scale CRISPR screens. Nature 535:159–163. https://doi.org/10.1038/nature18631.
11. Ooi YS, Majzoub K, Flynn RA, Mata MA, Diep J, Li JK, van Buuren N, Rumachik N, Johnson AG, Puschnik AS, Marceau CD, Mlera L, Grabowski JM, Kirkegaard K, Bloom ME, Sarnow P, Bertozzi CR, Carette JE. 2019. An RNA-centric dissection of host complexes controlling flavivirus infection. Nat Microbiol 4:2369–2382. https://doi.org/10.1038/s41564-019-0518-2.
12. Neufeldt CJ, Cortese M, Acosta EG, Bartenschlager R. 2018. Rewiring cellular networks by members of the Flaviviridae family. Nat Rev Microbiol 16:125–142. https://doi.org/10.1038/nrmicro.2017.170.
13. Mohorko E, Glockshuber R, Aebi M. 2011. Oligosaccharyltransferase: the central enzyme of N-linked protein glycosylation. J Inherit Metab Dis 34:869–878. https://doi.org/10.1007/s10545-011-9337-1.
14. Shurtleff MJ, Itzhak DN, Hussmann JA, Schirle Oakdale NT, Costa EA, Jonikas M, Weibezahn J, Popova KD, Jan CH, Sinitcyn P, Vembar SS, Hernandez H, Cox J, Burlingame AL, Brodsky JL, Frost A, Borner GH, Weissman JS, Shurtleff MJ, Itzhak DN, Hussmann JA, Schirle Oakdale NT, Costa EA, Jonikas M, Weibezahn J, Popova KD, Jan CH, Sinitcyn P, Vembar SS, Hernandez H, Cox J, Burlingame AL, Brodsky JL, Frost A, Borner GHH, Weissman JS. 2018. The ER membrane protein complex interacts cotranslationally to enable biogenesis of multipass membrane proteins. Elife 7:e37018. https://doi.org/10.7554/eLife.37018.
15. Guna A, Volkmar N, Christianson JC, Hegde RS. 2018. The ER membrane protein complex is a transmembrane domain insertase. Science 359:470–473. https://doi.org/10.1126/science.aao3099.
16. Pfeffer S, Dudek J, Schaffer M, Ng BG, Albert S, Plitzko JM, Baumeister W, Zimmermann R, Freeze HH, Engel BD, Forster F. 2017. Dissecting the molecular organization of the translocon-associated protein complex. Nat Commun 8:14516. https://doi.org/10.1038/ncomms14516.
17. Li Y, Muffat J, Omer Javed A, Keys HR, Lungjangwa T, Bosch I, Khan M, Virgilio MC, Gehrke L, Sabatini DM, Jaenisch R. 2019. Genome-wide CRISPR screen for Zika virus resistance in human neural cells. Proc Natl Acad Sci U S A 116:9527–9532. https://doi.org/10.1073/pnas.1900867116.
18. Savidis G, McDougall WM, Meraner P, Perreira JM, Portmann JM, Trincucci G, John SP, Aker AM, Renzette N, Robbins DR, Guo Z, Green S, Kowalik TF, Brass AL. 2016. Identification of Zika virus and dengue virus dependency factors using functional genomics. Cell Rep 16:232–246. https://doi.org/10.1016/j.celrep.2016.06.028.
19. Zhang R, Miner JJ, Gorman MJ, Rausch K, Ramage H, White JP, Zuiani A, Zhang P, Fernandez E, Zhang Q, Dowd KA, Pierson TC, Cherry S, Diamond MS. 2016. A CRISPR screen defines a signal peptide processing pathway required by flaviviruses. Nature 535:164–168. https://doi.org/10.1038/nature18625.
20. Shalem O, Sanjana NE, Hartenian E, Shi X, Scott DA, Mikkelson T, Heckl D, Ebert BL, Root DE, Doench JG, Zhang F. 2014. Genome-scale CRISPR-Cas9 knockout screening in human cells. Science 343:84–87. https://doi.org/10.1126/science.1247005.
21. Li W, Xu H, Xiao T, Cong L, Love MI, Zhang F, Irizarry RA, Liu JS, Brown M, Liu XS. 2014. MAGeCK enables robust identification of essential genes from genome-scale CRISPR/Cas9 knockout screens. Genome Biol 15:554. https://doi.org/10.1186/s13059-014-0554-4.
22. Colussi PA, Taron CH, Mack JC, Orlean P. 1997. Human and Saccharomyces cerevisiae dolichol phosphate mannose synthases represent two classes of the enzyme, but both function in Schizosaccharomyces pombe. Proc Natl Acad Sci U S A 94:7873–7878. https://doi.org/10.1073/pnas.94.15.7873.
23. Maeda Y, Kinoshita T. 2008. Dolichol-phosphate mannose synthase: structure, function and regulation. Biochim Biophys Acta 1780:861–868. https://doi.org/10.1016/j.bbagen.2008.03.005.
24. Ashida H, Maeda Y, Kinoshita T. 2006. DPM1, the catalytic subunit of dolichol-phosphate mannose synthase, is tethered to and stabilized on the endoplasmic reticulum membrane by DPM3. J Biol Chem 281:896–904. https://doi.org/10.1074/jbc.M511311200.
25. Maeda Y, Tanaka S, Hino J, Kangawa K, Kinoshita T. 2000. Human dolichol-phosphate-mannose synthase consists of three subunits, DPM1, DPM2 and DPM3. EMBO J 19:2475–2482. https://doi.org/10.1093/emboj/19.11.2475.
26. Gandini R, Reichenbach T, Tan TC, Divne C. 2017. Structural basis for dolichylphosphate mannose biosynthesis. Nat Commun 8:120. https://doi.org/10.1038/s41467-017-00187-2.
27. Aebi M, Gassenhuber J, Domdey H, te Heesen S. 1996. Cloning and characterization of the ALG3 gene of Saccharomyces cerevisiae. Glycobiology 6:439–444. https://doi.org/10.1093/glycob/6.4.439.
28. Maeda Y, Watanabe R, Harris CL, Hong Y, Ohishi K, Kinoshita K, Kinoshita T. 2001. PIG-M transfers the first mannose to glycosylphosphatidylinositol on the lumenal side of the ER. EMBO J 20:250–261. https://doi.org/10.1093/emboj/20.1.250.
29. Manya H, Chiba A, Yoshida A, Wang X, Chiba Y, Jigami Y, Margolis RU, Endo T. 2004. Demonstration of mammalian protein O-mannosyltransferase activity: coexpression of POMT1 and POMT2 required for enzymatic activity. Proc Natl Acad Sci U S A 101:500–505. https://doi.org/10.1073/pnas.0307228101.
30. Esapa CT, Bentham GR, Schroder JE, Kroger S, Blake DJ. 2003. The effects of post-translational processing on dystroglycan synthesis and trafficking. FEBS Lett 555:209–216. https://doi.org/10.1016/s0014-5793(03)01230-4.

31. Dejarnac O, Hafirassou ML, Chazal M, Versapuech M, Gaillard J, Perera-Lecoin M, Umana-Diaz C, Bonnet-Madin L, Carnec X, Tinevez JY, Delaugerre C, Schwartz O, Roingeard P, Jouvenet N, Berlioz-Torrent C, Meertens L, Amara A. 2018. TIM-1 ubiquitination mediates dengue virus entry. Cell Rep 23:1779–1793. https://doi.org/10.1016/j.celrep.2018.04.013.
32. Fischl W, Bartenschlager R. 2013. High-throughput screening using dengue virus reporter genomes. Methods Mol Biol 1030:205–219. https://doi.org/10.1007/978-1-62703-484-5_17.
33. Scaturro P, Cortese M, Chatel-Chaix L, Fischl W, Bartenschlager R. 2015. Dengue virus non-structural protein 1 modulates infectious particle production via interaction with the structural proteins. PLoS Pathog 11:e1005277. https://doi.org/10.1371/journal.ppat.1005277.
34. Cueva R, Munoz MD, Andaluz E, Basco RD, Larriba G. 1996. Preferential transfer to truncated oligosaccharides to the first sequon of yeast exo-glucanase in Saccharomyces cerevisiae alg3 cells. Biochim Biophys Acta 1289:336–342. https://doi.org/10.1016/0304-4165(95)00171-9.
35. Imbach T, Schenk B, Schollen E, Burda P, Stutz A, Grunewald S, Bailie NM, King MD, Jaeken J, Matthijs G, Berger EG, Aebi M, Hennet T. 2000. Deficiency of dolichol-phosphate-mannose synthase-1 causes congenital disorder of glycosylation type Ie. J Clin Invest 105:233–239. https://doi.org/10.1172/JCI8691.
36. Korner C, Knauer R, Stephani U, Marquardt T, Lehle L, von Figura K. 1999. Carbohydrate deficient glycoprotein syndrome type IV: deficiency of dolichyl-P-Man:Man(5)GlcNAc(2)-PP-dolichyl mannosyltransferase. EMBO J 18:6816–6822. https://doi.org/10.1093/emboj/18.23.6816.
37. Yap SSL, Nguyen-Khuong T, Rudd PM, Alonso S. 2017. Dengue virus glycosylation: what do we know? Front Microbiol 8:1415. https://doi.org/10.3389/fmicb.2017.01415.
38. Hebert DN, Lamriben L, Powers ET, Kelly JW. 2014. The intrinsic and extrinsic effects of N-linked glycans on glycoproteostasis. Nat Chem Biol 10:902–910. https://doi.org/10.1038/nchembio.1651.
39. Shi X, Brauburger K, Elliott RM. 2005. Role of N-linked glycans on Bunyamwera virus glycoproteins in intracellular trafficking, protein folding, and virus infectivity. J Virol 79:13725–13734. https://doi.org/10.1128/JVI.79.21.13725-13734.2005.
40. Shi X, Elliott RM. 2004. Analysis of N-linked glycosylation of Hantaan virus glycoproteins and the role of oligosaccharide side chains in protein folding and intracellular trafficking. J Virol 78:5414–5422. https://doi.org/10.1128/jvi.78.10.5414-5422.2004.
41. Zai J, Mei L, Wang C, Cao S, Fu ZF, Chen H, Song Y. 2013. N-glycosylation of the premembrane protein of Japanese encephalitis virus is critical for folding of the envelope protein and assembly of virus-like particles. Acta Virol 57:27–33. https://doi.org/10.4149/av_2013_01_27.
42. Lai CY, Tsai WY, Lin SR, Kao CL, Hu HP, King CC, Wu HC, Chang GJ, Wang WK. 2008. Antibodies to envelope glycoprotein of dengue virus during the natural course of infection are predominantly cross-reactive and recognize epitopes containing highly conserved residues at the fusion loop of domain II. J Virol 82:6631–6643. https://doi.org/10.1128/JVI.00316-08.
43. Puttikhunt C, Keelapang P, Khemnu N, Sittisombut N, Kasinrerk W, Malasit P. 2008. Novel anti-dengue monoclonal antibody recognizing conformational structure of the prM-E heterodimeric complex of dengue virus. J Med Virol 80:125–133. https://doi.org/10.1002/jmv.21047.
44. Zheng A, Umashankar M, Kielian M. 2010. In vitro and in vivo studies identify important features of dengue virus pr-E protein interactions. PLoS Pathog 6:e1001157. https://doi.org/10.1371/journal.ppat.1001157.
45. Bradel-Tretheway BG, Liu Q, Stone JA, McInally S, Aguilar HC. 2015. Novel functions of Hendra virus G N-glycans and comparisons to Nipah virus. J Virol 89:7235–7247. https://doi.org/10.1128/JVI.00773-15.
46. Julithe R, Abou-Jaoudé G, Sureau C. 2014. Modification of the hepatitis B virus envelope protein glycosylation pattern interferes with secretion of viral particles, infectivity, and susceptibility to neutralizing antibodies. J Virol 88:9049–9059. https://doi.org/10.1128/JVI.01161-14.
47. Lavie M, Hanoulle X, Dubuisson J. 2018. Glycan shielding and modulation of hepatitis C virus neutralizing antibodies. Front Immunol 9:910. https://doi.org/10.3389/fimmu.2018.00910.
48. Sodora DL, Cohen GH, Eisenberg RJ. 1989. Influence of asparagine-linked oligosaccharides on antigenicity, processing, and cell surface expression of herpes simplex virus type 1 glycoprotein D. J Virol 63:5184–5193. https://doi.org/10.1128/JVI.63.12.5184-5193.1989.
49. Watterson D, Modhiran N, Young PR. 2016. The many faces of the flavivirus NS1 protein offer a multitude of options for inhibitor design. Antiviral Res 130:7–18. https://doi.org/10.1016/j.antiviral.2016.02.014.
50. Pryor MJ, Gualano RC, Lin B, Davidson AD, Wright PJ. 1998. Growth restriction of dengue virus type 2 by site-specific mutagenesis of virus-encoded glycoproteins. J Gen Virol 79:2631–2639. https://doi.org/10.1099/0022-1317-79-11-2631.
51. Crabtree MB, Kinney RM, Miller BR. 2005. Deglycosylation of the NS1 protein of dengue 2 virus, strain 16681: construction and characterization of mutant viruses. Arch Virol 150:771–786. https://doi.org/10.1007/s00705-004-0430-8.
52. Tajima S, Takasaki T, Kurane I. 2008. Characterization of Asn130-to-Ala mutant of dengue type 1 virus NS1 protein. Virus Genes 36:323–329. https://doi.org/10.1007/s11262-008-0211-7.
53. Whiteman MC, Popov V, Sherman MB, Wen J, Barrett AD. 2015. Attenuated West Nile virus mutant NS1130-132QQA/175A/207A exhibits virus-induced ultrastructural changes and accumulation of protein in the endoplasmic reticulum. J Virol 89:1474–1478. https://doi.org/10.1128/JVI.02215-14.
54. Hafirassou ML, Meertens L, Umana-Diaz C, Labeau A, Dejarnac O, Bonnet-Madin L, Kummerer BM, Delaugerre C, Roingeard P, Vidalain PO, Amara A. 2017. A global interactome map of the dengue virus NS1 identifies virus restriction and dependency host factors. Cell Rep 21:3900–3913. https://doi.org/10.1016/j.celrep.2017.11.094.
55. Frenkel Z, Gregory W, Kornfeld S, Lederkremer GZ. 2003. Endoplasmic reticulum-associated degradation of mammalian glycoproteins involves sugar chain trimming to Man6-5GlcNAc2. J Biol Chem 278:34119–34124. https://doi.org/10.1074/jbc.M305929200.
56. Cherepanova N, Shrimal S, Gilmore R. 2016. N-linked glycosylation and homeostasis of the endoplasmic reticulum. Curr Opin Cell Biol 41:57–65. https://doi.org/10.1016/j.ceb.2016.03.021.
57. Hanna SL, Pierson TC, Sanchez MD, Ahmed AA, Murtadha MM, Doms RW. 2005. N-linked glycosylation of West Nile virus envelope proteins influences particle assembly and infectivity. J Virol 79:13262–13274. https://doi.org/10.1128/JVI.79.21.13262-13274.2005.
58. Kim JM, Yun SI, Song BH, Hahn YS, Lee CH, Oh HW, Lee YM. 2008. A single N-linked glycosylation site in the Japanese encephalitis virus prM protein is critical for cell type-specific prM protein biogenesis, virus particle release, and pathogenicity in mice. J Virol 82:7846–7862. https://doi.org/10.1128/JVI.00789-08.
59. Mondotte JA, Lozach PY, Amara A, Gamarnik AV. 2007. Essential role of dengue virus envelope protein N glycosylation at asparagine-67 during viral propagation. J Virol 81:7136–7148. https://doi.org/10.1128/JVI.00116-07.
60. Meertens L, Carnec X, Lecoin MP, Ramdasi R, Guivel-Benhassine F, Lew E, Lemke G, Schwartz O, Amara A. 2012. The TIM and TAM families of phosphatidylserine receptors mediate dengue virus entry. Cell Host Microbe 12:544–557. https://doi.org/10.1016/j.chom.2012.08.009.
61. Meertens L, Hafirassou ML, Couderc T, Bonnet-Madin L, Kril V, Kummerer BM, Labeau A, Brugier A, Simon-Loriere E, Burlaud-Gaillard J, Doyen C, Pezzi L, Goupil T, Rafasse S, Vidalain PO, Bertrand-Legout A, Gueneau L, Juntas-Morales R, Ben Yaou R, Bonne G, de Lamballerie X, Benkirane M, Roingeard P, Delaugerre C, Lecuit M, Amara A. 2019. FHL1 is a major host factor for chikungunya virus infection. Nature 574:259–263. https://doi.org/10.1038/s41586-019-1578-4.
62. Carnec X, Meertens L, Dejarnac O, Perera-Lecoin M, Hafirassou ML, Kitaura J, Ramdasi R, Schwartz O, Amara A. 2016. The phosphatidylserine and phosphatidylethanolamine receptor CD300a binds dengue virus and enhances infection. J Virol 90:92–102. https://doi.org/10.1128/JVI.01849-15.